

Structural and electronic effects induced by carboxylic acid substitution in isomeric 2,2'-bithiophenes and oligothiophenes: A computational study

Jordi Casanovas^{a,*}, David Zanuy^b, Carlos Alemán^{b,*}

^aDepartament de Química, Escola Politècnica Superior, Universitat de Lleida, c/Jaume II no 69, Lleida E-25001, Spain

^bDepartament d'Enginyeria Química, E.T.S. d'Enginyers Industrials de Barcelona, Universitat Politècnica de Catalunya, Diagonal 647, Barcelona E-08028, Spain

Received 3 May 2005; received in revised form 7 July 2005; accepted 9 July 2005

Available online 9 August 2005

Abstract

The structural and electronic properties of carboxylic acid-substituted 2,2'-bithiophenes have been examined using quantum mechanical methods based on density functional theory. Calculations at the B3PW91/6-31+G(d,p) level were performed on 2,2'-bithiophene-4,4'-dicarboxylic acid, 2,2'-bithiophene-3,4'-dicarboxylic acid and 2,2'-bithiophene-3,3'-dicarboxylic acid, different arrangements being additionally considered for the carboxylic acid substituents of each isomer. The energy gap calculated for 2,2'-bithiophene-3,4'-dicarboxylic acid was about 0.15 eV smaller than that predicted for unsubstituted 2,2'-bithiophene. Additional calculations were performed on oligothiophenes containing n carboxylic acid substituted thiophene rings, n ranging from 2 to 7. The results, which allowed to estimate the band gap for the corresponding poly(thiophene carboxylic acid)s, indicated that the introduction of carboxylic acid substituents at polythiophene produces a very small increase in the ϵ_g gap.

© 2005 Elsevier Ltd. All rights reserved.

Keywords: Thiophene substitution; Carboxylic acid; Quantum chemical calculations

1. Introduction

The electrical and optical properties of organic conjugated polymers have attracted much interest from both technological and fundamental points of view. A potential advantage of these polyconjugated materials is that their electronic structure, and consequently their properties, can be modulated at the molecular level by introducing side chains with suitable functionalities. Thus, the electronic and/or steric effects produced by the incorporation of substituents at the right positions usually result in an improvement of the polymer characteristics.

Among organic conjugated polymers, polythiophene has received particular attention [1–3]. The main drawback of unsubstituted polythiophene is its lack of solubility, which explains its poor processability. Substitution on the

thiophene ring with relatively long and flexible alkyl chains produces soluble polymers in organic solvents [4–10]. The same strategy has been applied to produce water-soluble polythiophenes by incorporating hydrophilic substituents [11–17]. In particular, the introduction of carboxylic acid substituents at the 3-position of the thiophene ring has provided water-soluble conducting polymers with interesting electrical and optical properties [11–17]. Thus, carboxylic acid functionality induces not only water solubility but also complicated electronic interactions with the π -system of polythiophene.

In recent studies, Pomerantz and co-workers [18–20] investigated the role of the carboxylate group on the structure of polythiophenes containing ester functionalities. However, the effects of the interactions between the side chain functionality and the polymer backbone have not been examined yet for poly(thiophene carboxylic acid)s, hereafter denoted PTCAs, nor their model compounds. It should be emphasized that, due their obvious chemical differences, the influence of the carboxylate group on the polymer structure is expected to be different for ester and carboxylic acid functionalities.

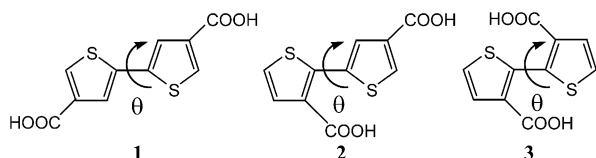
* Corresponding authors.

E-mail addresses: jcasanovas@quimica.udl.es (J. Casanovas), carlos.aleman@upc.es (C. Alemán).

In this work we describe how the carboxylic acid functionality of PTCAs affects the molecular and electronic structure of the polymer chain. For this purpose quantum chemical methods based on density functional theory (DFT) have been applied to model compounds formed by n carboxylic acid substituted thiophene rings, n ranging from 2 to 7. Results have been compared with those reported for ester substituted oligothiophenes [18–20].

2. Methods

In a first step, we examined three isomeric bithiophenes: 2,2'-bithiophene-4,4'-dicarboxylic acid (**1**), 2,2'-bithiophene-3,4'-dicarboxylic acid (**2**) and 2,2'-bithiophene-3,3'-dicarboxylic acid (**3**), which are models for tail-to-tail (t-t), tail-to-head (t-h) and head-to-head (h-h) PTCAs linkages.



The internal rotation was studied by scanning the inter-ring torsional angle θ in steps of 30° between $\theta = 180^\circ$ (*anti* conformer) and $\theta = 0^\circ$ (*syn* conformer). A flexible rotor approximation was used for all the compounds investigated. Thus, the structure in each point of the path was obtained from geometry optimization at a fixed θ value. For each compound, equilibrium geometries were fully optimized using a gradient method. All the minimum energy structures were characterized as such by calculating and diagonalizing the Hessian matrix and ensuring that they do not have any negative value.

Afterwards the variation of the electronic properties with the extension of the polymer chain was examined. For this purpose, geometry optimizations were performed on oligomers containing n substituted thiophene rings, with n ranging from 2 to 7, and different types of t-t, t-h and h-h linkages. An all-*anti* conformation was considered in all cases, i.e. all the inter-ring dihedral angles (θ_i , where i ranges from 1 to $n - 1$) were fixed at 180.0° during geometry optimizations.

Calculations of both dimers and n -oligomers were performed using the Becke's three-parameter hybrid functional [21] combined with the Perdew and Wang's correlation functional [22] (B3PW91), the 6-31+G(d,p) [23] basis set being used in all cases. Thus, preliminary calculations on 2,2'-bithiophene, hereafter abbreviated **bthp**, using different theoretical methods and basis sets (data not shown) indicated that the results provided by the B3PW91/6-31+G(d,p) level are in agreement with experimental data. The PC-Gamess [24] and Gaussian 98 [25] programs were used for the calculations.

Ionization potentials (IP) were estimated using the Koopman's theorem (KT) [26], i.e. relating the IP to the

energy of the HOMO (highest occupied molecular orbital), which according to the Janak's theorem can be also applied to DFT calculations [27,28]. Finally, the energy gap (ϵ_g) was evaluated as the difference between the HOMO and LUMO (lowest unoccupied molecular orbital) energies: $\epsilon_g = \epsilon_{\text{LUMO}} - \epsilon_{\text{HOMO}}$. In an early work, Levy et al. [28] showed that in DFT calculations ϵ_g can be rightly estimated using this procedure.

3. Results and discussion

3.1. 2,2'-Bithiophene-4,4'-dicarboxylic acid (**1**)

The structure of **1** is expected to depend on the arrangement of the two carboxylic acid groups. In order to examine the relation between the inter-ring dihedral angle θ and the arrangement of the side chains, the following 8 possibilities were considered:

Fig. 1 represents the quantum mechanical profiles for **1a–h** relative to the most stable conformation. As can be seen, the eight arrangements can be clearly categorized in three groups depending on their relative energies. In the most favored group, which contains **1a**, **1c** and **1e**, the repulsive interactions between the side chains and the hydrogens

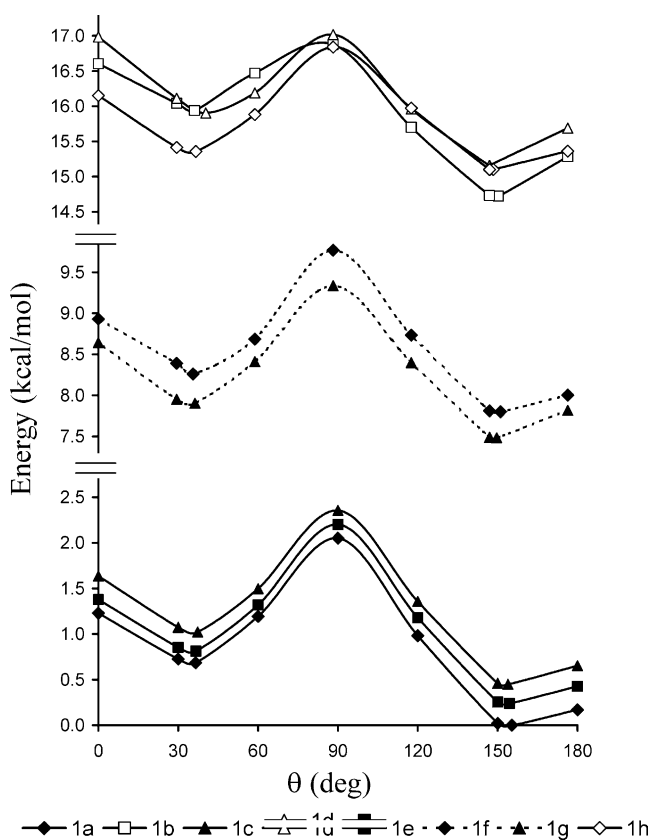
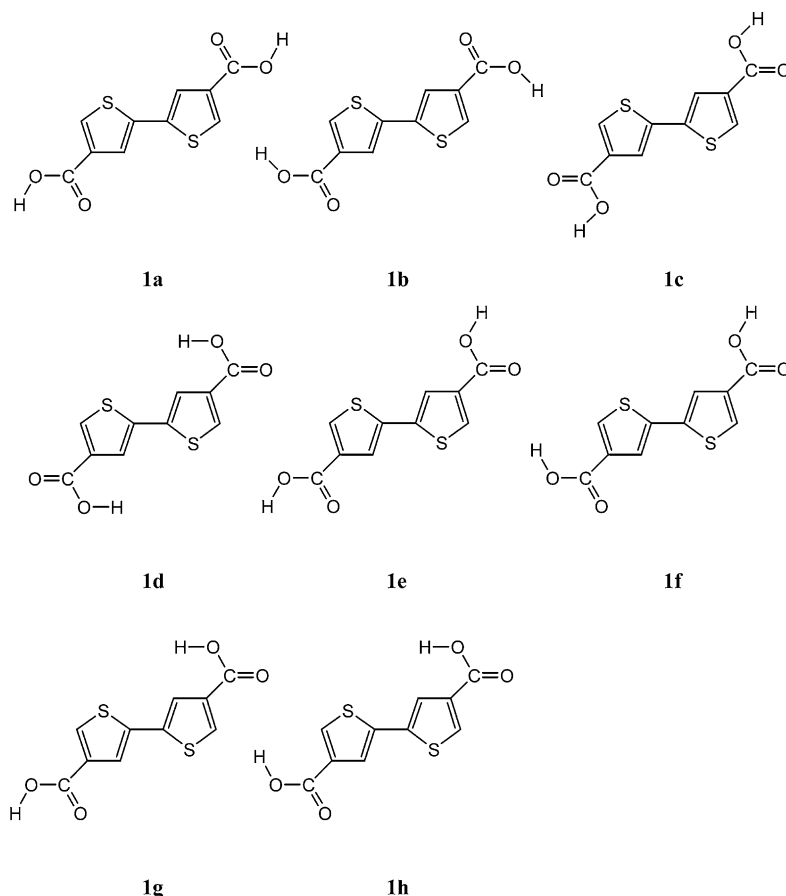
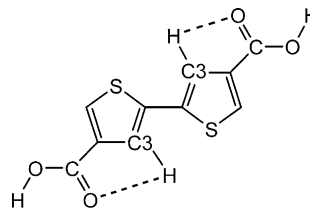


Fig. 1. Potential energy curves for the internal rotation of **1a–h** as a function of the inter-ring dihedral angle (θ) using B3PW91/6-31+G(d,p) optimizations. Energies are relative to the global minimum.



attached to the carbon atoms of the thiophene rings are minimum. Accordingly, the notable stabilization of these arrangements with respect to the other five cannot be attributed to any intense attractive interaction but to the lack of unfavorable steric clashes.

The most important difference among **1a**, **1c** and **1e** involves to the number of weakly attractive interactions between the C=O group of the side chains and the C3–H of the thiophene rings. These interactions remind those found for the extended conformation of nylons [29] and peptides [30], where the N–H group of an amide functionality interacts with the C=O group of consecutive one. Furthermore, the carbonyl oxygen of the carboxylate moiety was found to form stronger O···H interactions than the alkoxy oxygen [31]. The number of C=O···H–C3 interactions in **1a**, **1e** and **1c** is two, one and none, respectively, the relative stability of these arrangements being **1a** > **1e** > **1c**. Consistently, the H···O distance in C=O···H–C3 interactions (at **1a** and **1e**) is slightly larger than that of C=O···H–C5 interactions (at **1c** and **1e**). However, it should be noted that the three arrangements differ by less than 0.5 kcal/mol, which indicates that such relative energy order is actually governed by a balance between very weak interactions.



On the other hand, the least favored group of arrangements is formed by **1b**, **1d** and **1h**, which are destabilized with respect to **1a** by about 15–16 kcal/mol. All these arrangements present steric and electrostatic repulsive interactions between the hydrogen of the carboxylic acid groups and the hydrogen attached to C3 and/or C5 atoms. These intra-ring repulsions are illustrated in the following scheme for **1h**, where the repulsions with both C3 and C5 can be identified.

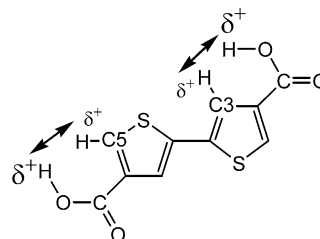


Table 1
Energies (in kcal/mol) and inter-ring dihedral angles (θ ; in deg) of **1a–g** and **bthp** computed at the B3PW91/6-31+G(d,p) level

	<i>anti</i> ^a	<i>anti-gauche</i>	<i>gauche-gauche</i> ^b	<i>syn-gauche</i>	<i>syn</i> ^c
1a	0.2	0.0 ($\theta=155.3^\circ$)	2.0	0.7 ($\theta=36.5^\circ$)	1.2
1b	0.6	0.0 ($\theta=153.4^\circ$)	2.2	0.8 ($\theta=36.9^\circ$)	1.9
1c	0.2	0.0 ($\theta=153.9^\circ$)	1.9	0.6 ($\theta=37.3^\circ$)	1.2
1d	0.5	0.0 ($\theta=149.9^\circ$)	1.9	0.7 ($\theta=41.2^\circ$)	1.8
1e	0.2	0.0 ($\theta=154.4^\circ$)	2.0	0.6 ($\theta=36.6^\circ$)	1.1
1f	0.2	0.0 ($\theta=154.2^\circ$)	2.0	0.4 ($\theta=36.3^\circ$)	1.1
1g	0.3	0.0 ($\theta=152.7^\circ$)	1.9	0.4 ($\theta=37.1^\circ$)	1.2
1h	0.3	0.0 ($\theta=151.5^\circ$)	1.7	0.3 ($\theta=37.4^\circ$)	1.0
Bthp	0.2	0.0 ($\theta=154.3^\circ$)	2.2	0.6 ($\theta=35.7^\circ$)	1.1

^a $\theta=180^\circ$.

^b $\theta=90^\circ$.

^c $\theta=0^\circ$.

Finally, in the group formed by **1f** and **1g** the conformation of the carboxylic acid side chains are halfway between those of the arrangements contained in the most and least favored groups. Accordingly, **1f** and **1g** are less favored than **1a** by about 8 kcal/mol.

The energies and torsional angles of the minima and saddle points obtained for the eight arrangements **1a–g** are compiled in Table 1, the results obtained for **bthp** at the same computational level being also included for comparison. Energies are relative to the global minimum predicted for every arrangement. As can be seen, the conformational preferences predicted for **1** are relatively independent of the conformation of the side chains. The global minimum predicted for every arrangement of **1** appears at $\theta \approx 150$ – 155° (*anti-gauche* conformation), a local minimum being detected at $\theta \approx 36$ – 41° (*syn-gauche* conformation). The latter is less stable than the global minimum by 0.3–0.8 kcal/mol. Both minima are separated by the *gauche-gauche* barrier at $\theta=90^\circ$. This is unfavored by about 1.7–2.2 and 1.2–1.6 kcal/mol with respect to the *anti-gauche* and *syn-gauche* minima, respectively. Finally, the *anti* barrier ($\theta=180^\circ$) separates the global minimum and its degenerated state at $\theta \approx -150^\circ$ while the *syn-gauche* minimum and its degenerated state at $\theta \approx -37^\circ$ are separated by the *syn* barrier ($\theta=0^\circ$). The *anti* and *syn* barriers are 1.4–1.8 and 0.1–0.9 kcal/mol lower in energy than the *gauche-gauche* one. On the other hand, comparison between **1** and **bthp** indicates that the introduction of carboxylic acid side chains at 4,4'-positions does not produce any relevant change in the conformational preferences.

Table 2 lists the inter-ring bond length (d), IP and ϵ_g predicted for the *anti-gauche* minimum of **1a–g** and **bthp**. As can be seen, the influence of the carboxylic acid side chains on d and ϵ_g is almost negligible. Indeed, the substituents reduce simultaneously the energy of both the HOMO and LUMO and, consequently, the gaps calculated for **1** and **bthp** remain similar. This is consistent with the shape of the HOMO and LUMO, which are displayed in Fig. 2 for the lowest energy minimum of **1a** and **bthp**, respectively. As can be seen, the contribution of the side groups to the frontier orbitals of **1a** is relatively small and

similar for both the HOMO and the LUMO. Consequently, these orbitals are quite similar for **1a** and **bthp**, being mainly localized at the thiophene units in both cases. The effect of the substitution on the energy of the HOMO is reflected by the IP, which is about 0.6–1.1 eV higher for **1** than for **bthp**. As expected from the shapes of the frontier

Table 2
Inter-ring bond length (d), ionization potential (IP) and energy gap (ϵ_g) of **1a–g** and **bthp** calculated at the B3PW91/6-31+G(d,p) level

	d (Å)	IP (eV)	ϵ_g (eV)
1a	1.451	6.48	4.36
1b	1.452	6.86	4.40
1c	1.451	6.50	4.35
1d	1.451	6.94	4.40
1e	1.451	6.49	4.35
1f	1.451	6.67	4.35
1g	1.451	6.71	4.38
1h	1.452	6.89	4.37
Bthp	1.451	5.88	4.35

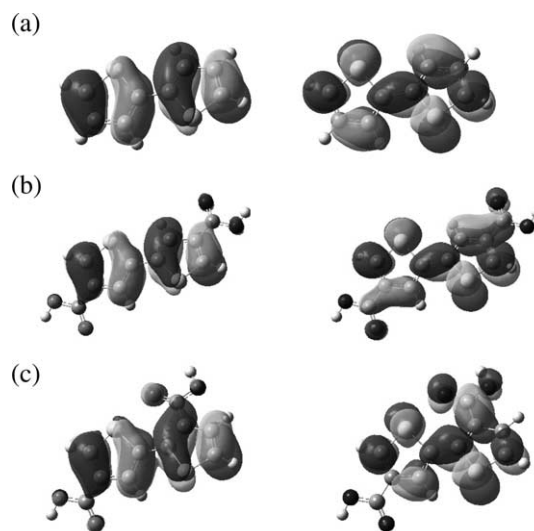
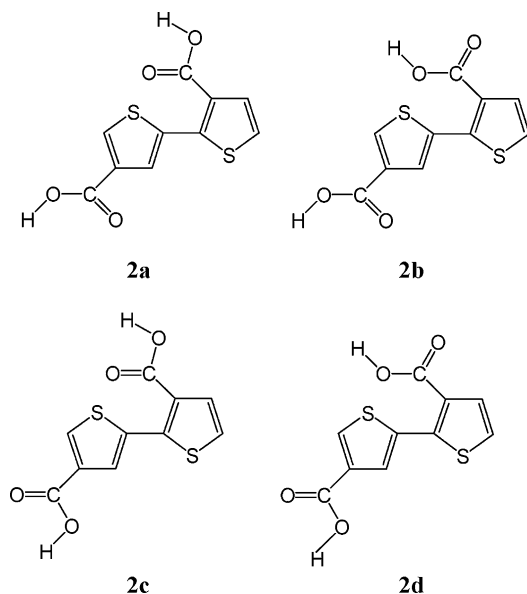


Fig. 2. HOMO (left) and LUMO (right) at isosurfaces of 0.02 of (a) **bthp**, (b) **1a** and (c) **2a**.

orbitals, arrangement **1a** provided the smallest difference with respect to **bthp** (0.6 eV).

3.2. 2,2'-Bithiophene-3,4'-dicarboxylic acid (**2**)

Taking into account the results obtained for **1**, only 4 different arrangements were considered for the carboxylic acid side chains of **2**:



However, the low stability of all the other arrangements was confirmed by calculating the most stable minimum of every one (data not shown). The rotational profiles calculated for **2a–d** are displayed in Fig. 3(a), while Table 3 lists the relative energies and inter-ring dihedral angles of the minimum energy conformations and the barriers. The energies represented in Fig. 3(a), which are relative to the global minimum of the most stable arrangement of **1**, indicate that the latter isomer is around 4 kcal/mol more stable than **2**. Furthermore, a detailed inspection of the result reveals that the conformational preferences of **2a** and **2c** are similar to those described above for **1a–h**. Thus, although substitution at the C3-position produces more repulsive interactions than at C4, these are not strong enough to induce drastic changes in the conformational preferences if the carbonyl oxygen points to the sulphur atom of the adjacent ring. In opposition, if the alkoxy oxygen atom of the carboxylic acid group attached to C3 points to the

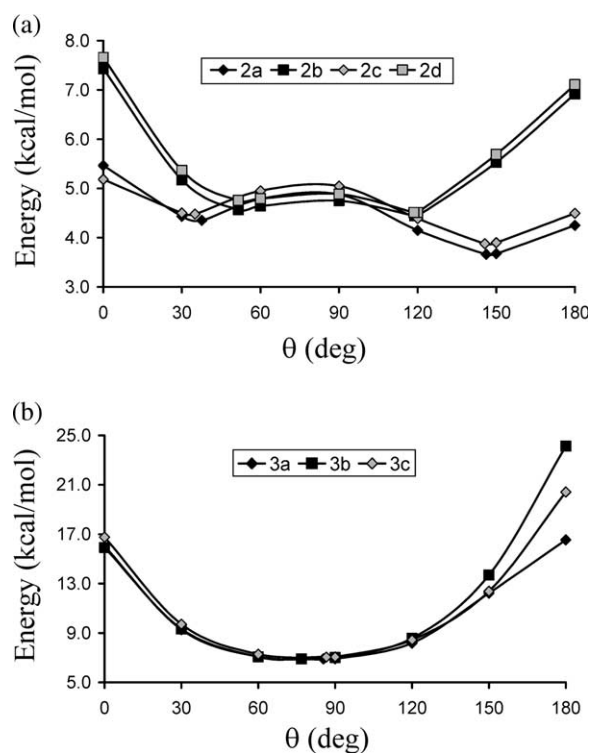


Fig. 3. Potential energy curves for the internal rotation of (a) **2a–d** and (b) **3a–c** as a function of the inter-ring dihedral angle (θ) using B3PW91/6-31+G(d,p) optimizations. Energies are relative to the global minimum of isomer **1**.

sulphur atom of the contiguous thiophene ring, as occurs in **2b** and **2d**, strong repulsive interactions are produced. These features are due to the electron lone pairs localized at the oxygen atoms, which present different spatial orientations in the alkoxy and carbonyl oxygen atoms.

The conformational distortions produced by the repulsive interactions in **2b** and **2d** can be summarized as follows: (a) the inter-ring dihedral angle of the *anti-gauche* minimum is around 27° smaller than for **2a** and **2c**; (b) the energy of the minima and the *gauche–gauche* barrier differ by less than 0.4 kcal/mol. Accordingly, the potential energy surface $E = E(\theta)$ is very flat in the range from $\theta \approx 52–119^\circ$, where the repulsive interactions generated by the carboxylic acid group attached to C3 are minimized.

Table 4 displays the inter-ring bond length and electronic properties for the *anti-gauche* minimum of **2a–d**. Interestingly, the energy gaps of **2a** and **2c** decrease by almost

Table 3
Energies (in kcal/mol) and inter-ring dihedral angles (θ ; in deg) of **2a–d** computed at the B3PW91/6-31+G(d,p) level

	<i>anti</i> ^a	<i>anti-gauche</i>	<i>gauche–gauche</i> ^b	<i>syn-gauche</i>	<i>syn</i> ^c
2a	0.6	0.0 ($\theta = 146.2^\circ$)	1.2	0.7 ($\theta = 37.6^\circ$)	1.8
2b	2.5	0.0 ($\theta = 118.9^\circ$)	0.3	0.1 ($\theta = 51.6^\circ$)	3.0
2c	0.6	0.0 ($\theta = 145.6^\circ$)	1.2	0.6 ($\theta = 35.2^\circ$)	1.3
2d	2.6	0.0 ($\theta = 118.6^\circ$)	0.4	0.2 ($\theta = 51.6^\circ$)	3.1

^a $\theta = 180^\circ$.

^b $\theta = 90^\circ$.

^c $\theta = 0^\circ$.

Table 4
Inter-ring bond length (d), ionization potential (IP) and energy gap (ϵ_g) of **2a–d** calculated at the B3PW91/6-31+G(d,p) level

	d (Å)	IP (eV)	ϵ_g (eV)
2a	1.456	6.44	4.19
2b	1.461	6.77	4.61
2c	1.456	6.45	4.17
2d	1.461	6.78	4.60

0.2 eV with respect to those of **1a–g**. This is produced by significant contribution of the carboxylic group linked at C4 to the LUMO of **2a** and **2c**, as is evidenced for the former arrangement in Fig. 2(c). On the other hand, the HOMO of **1a** and **2a** (Fig. 2(b) and (c), respectively) are notably similar, justifying that the IP remains essentially unaltered when one of the substituents changes from C4 to C3. On the other hand, the repulsive interactions of **2b** and **2d** result in an increase of both the inter-ring bond length and ϵ_g , which are consistent with the changes in ϵ discussed above for the *anti-gauche* and *syn-gauche* minima.

3.3. 2,2'-Bithiophene-3,3'-dicarboxylic acid (**3**)

The arrangements investigated for the carboxylic acid side chains of **3** were:

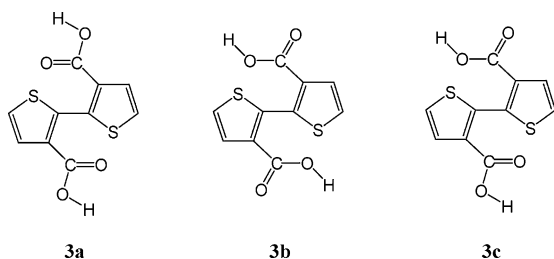


Fig. 3(b) shows the rotation profiles computed for **3a–c**, the represented energies being relative to the global minimum of **1**. As can be seen, **3** is unfavored with respect to **1a** by about 7 kcal/mol, independently of the arrangement of the side chains. Furthermore, the most stable conformation of **3a–c** is the *gauche–gauche* rather than the *anti-gauche* as was found above for **1a–h**, **2a–d** and **bthp**. The *syn* conformation is around 9 kcal/mol less stable than the *gauche–gauche* one (Table 5) independently of the arrangement of the acid side chains, while the relative stability of the *anti* conformation ranges from 9.6 (**3a**) to 17.2 kcal/mol (**3b**). The reason for these conformational preferences has to be found in the repulsive steric interactions generated by the substituents. These interactions are minimized when the θ dihedral angle change from 0° (*syn*) or 180° (*anti*) to $76–86^\circ$.

The influence of the loss of planarity on the electronic properties is clearly showed in Table 6. Thus, ϵ_g is 0.6–0.7 eV higher for the *gauche–gauche* minimum of **3a–c** than for the *anti-gauche* minimum of **1a–h**. Moreover, the inter-

Table 5
Energies (in kcal/mol) and inter-ring dihedral angles (θ ; in deg) of **3a–d** computed at the B3PW91/6-31+G(d,p) level

	<i>anti</i> ^a	<i>gauche–gauche</i>	<i>syn</i> ^b
3a	9.6	0.0 ($\theta=85.4^\circ$)	9.1
3b	17.2	0.0 ($\theta=76.8^\circ$)	9.0
3c	13.4	0.0 ($\theta=86.6^\circ$)	9.7

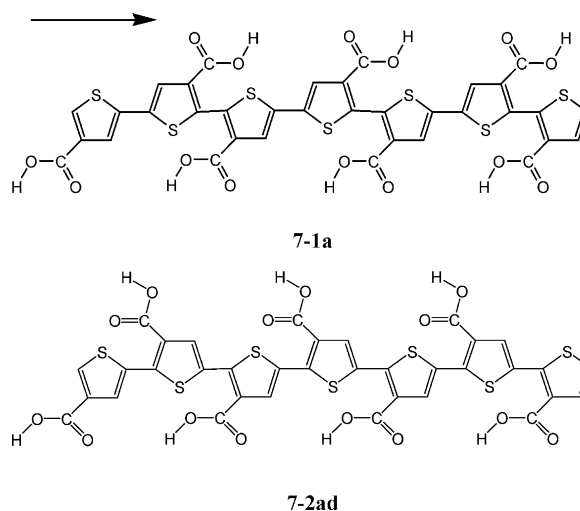
^a $\theta=180^\circ$.

^b $\theta=0^\circ$.

ring bond length is larger for isomer **3** than for **1** and **2** by about 0.010 and 0.005 Å, respectively, which is consistent with the smaller inter-annular π -conjugation of the former.

3.4. *n*-Oligothiophene carboxylic acids

In order to examine the evolution of the structural and electronic properties with the number of thiophene rings (n), calculations have been performed on *n*-oligomers with n ranging from 2 to 7. The side groups were arranged according to the results obtained for the isomeric bithiophene carboxylic acids **1–3**. Two different cases were considered that, for $n=7$, consist on:



The arrow shows the growing direction of the chains, i.e. the repeating units are added following the direction indicated by the arrow. The first set of compounds, denoted *n-1a*, was obtained by linking bithiophenes with the side

Table 6
Inter-ring bond length (d), ionization potential (IP) and energy gap (ϵ_g) of **3a–c** calculated at the B3PW91/6-31+G(d,p) level

	d (Å)	IP (eV)	ϵ_g (eV)
3a	1.465	6.87	5.08
3b	1.466	6.97	4.90
3c	1.466	6.96	5.08

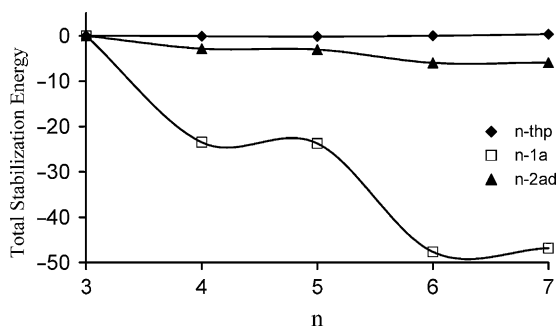


Fig. 4. Total stabilization energy (in kcal/mol) from long-range interactions in *n-thp*, *n-1a* and *n-2ad* oligomers.

groups arranged as in **1a**. As can be seen from the scheme of **7-1a**, this pattern of repetition produces a set of compounds that consists on combination of **1a**, which is the lowest energy arrangement of the t–t isomer **1**, and **3b**, which is practically isoenergetic to the other arrangements of the h–h isomer **3**. The second set of compounds has been denoted *n-2ad* and arises from the repetition of **2a**, which is the most stable arrangement of the t–h isomer **2**. As a consequence of the enlargement of the chain, a regular mix of **2a** and **2d** arrangements appears for $n > 2$. Furthermore, in order to ascertain the influence of the carboxylic acid groups on the analyzed properties, additional calculations were carried out on *n*-oligomers constituted by unsubstituted thiophene rings (*n-thp*).

Geometry optimizations at the B3PW91/6-31+G(d,p) level of *n-1a*, *n-2ad* and *n-thp*, where n ranges from 2 to 7, were performed for the *anti* conformation, i.e. all the inter-ring dihedral angles S–C–C–S were fixed at 180° . The importance of long-range interactions in the stabilization of oligomer chains was investigated by examining the stabilization energy (ΔE_{stab}), which was defined as the energy gain obtained upon the addition of the n th unit to the oligomer formed by $n-1$ units with respect to the energy gain of the formation of the oligomer with $n=3$ from that with $n=2$. Thus, for an oligomer formed by n units, ΔE_{stab}

was computed as,

$$\Delta E_{\text{stab}} = (E_n - E_{n-1}) - (E_3 - E_2) \quad (1)$$

where E_n , E_{n-1} , E_3 and E_2 are the energies of the oligomers constituted by n , $n-1$, 3 and 2 units, respectively. It should be noted that the energy difference ($E_3 - E_2$) corresponds to the change of energy at the formation of the oligomer formed by three units, which is free from long-range effects.

Fig. 4 shows the gradual variation with n of the total stabilization energy, which was estimated summing up the individuals values of ΔE_{stab} from oligomers with $n=4$ to oligomers with $n=7$ for *n-1a*, *n-2ad* and *n-thp*. It is worth noting that the stabilization due to long-range interactions is almost negligible for *n-thp*. Thus, the total stabilization in the longest oligomer is almost null (0.4 kcal/mol). On the other hand, inspection to the results obtained for *n-1a* reveals the presence of important long-range interactions. The stabilization upon the addition of a structural unit starts with -23.5 kcal/mol for **4-1a**, remains more or less constant for **5-1a**, increases suddenly to -47.6 kcal/mol for **6-1a** and, finally, again no extra stabilization appears for **7-1a**. These results indicate that t–t linkages produce a very large stabilization, i.e. about -23.5 kcal/mol, while the h–h linkages do not produce any energy gain. Regarding to *n-2ad*, results reveal a small but non-negligible stabilization. Thus, the total stabilization for **7-2ad** is -5.9 kcal/mol indicating that the incorporation of substituents bearing a carboxylic acid group produce an energy gain not only in the most favored t–t linkages but also in the h–t ones. Furthermore, a detailed analysis of the results indicates that this stabilization depends on the arrangement of the carboxylic acid groups. Thus, the stabilization associated to the **2a** and **2d** arrangements is -2.7 and -0.1 kcal/mol, respectively.

Fig. 5 represents the evolution of ϵ_g with inverse chain length ($1/n$) for the three systems. Interestingly, *n-thp* and *n-2ad* shows an almost perfect linear behavior ($y=ax+b$),

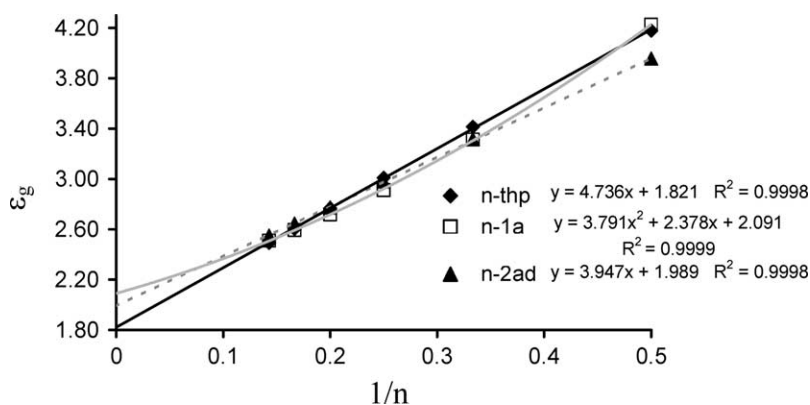


Fig. 5. Evolution of ϵ_g with inverse chain length ($1/n$) for *n-thp*, *n-1a* and *n-2ad* oligomers. The solid lines are linear (*n-thp* and *n-2ad*) and polynomial (*n-1a*) regressions with the formula and fit given.

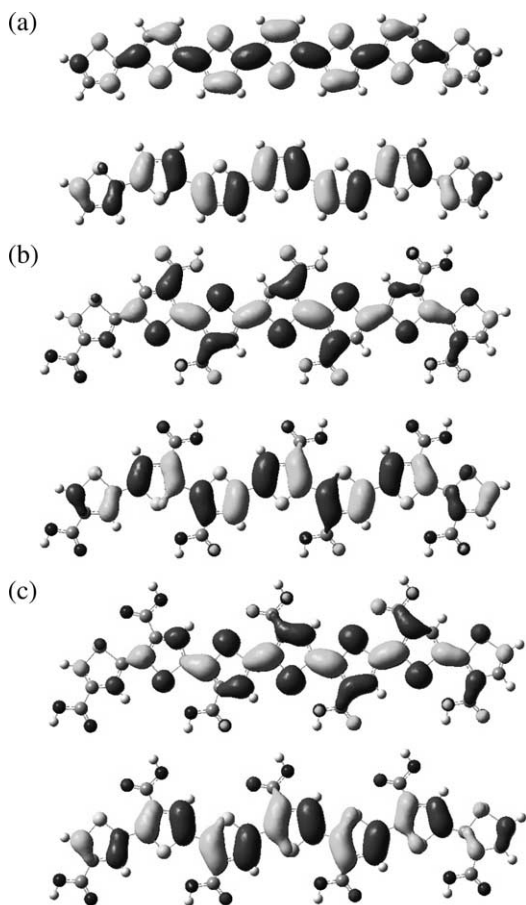


Fig. 6. HOMO (down) and LUMO (top) at isosurfaces of 0.02 of (a) **7-thp**, (b) **7-1a** and (c) **7-2ad**.

while **n-1a** presents a more complex polynomial behavior ($y = ax^2 + bx + c$) due to the alternative disposition of t–t and h–h linkages. Using these relationships, ϵ_g gaps of 1.82, 2.09 and 1.99 eV are extrapolated for infinite chain of **n-thp**, **n-1a** and **n-2ad**, respectively. The prediction for the former compound is in excellent agreement with the value electrochemically measured for poly(thiophene) (~ 2.0 eV) [32,33]. Comparison between the three types of oligothiophenes indicates that the carboxylic acid side groups reduce the energy of both the HOMO and the LUMO, the stabilization of the former is slightly greater than that of the latter.

The overall of these results can be understood by looking at Fig. 6, which shows the shapes of the HOMO and LUMO for **7-thp**, **7-1a** and **7-2ad**. As can be seen, the influence of the carboxylic acid side chains is very small in the HOMO of **7-1a** and **7-2ad**, the shape of the orbital remaining essentially unaltered with respect to that of **7-thp**. On the other hand, the carbon atom of the carboxylic acid groups contributes to the LUMO of **7-1a** and **7-2ad** indicating a certain delocalization from the conjugated backbone to the side chains. However, for the three oligomers the LUMO favors the inter-ring mobility

of electrons, while the HOMO only promotes the intraring mobility of electrons.

In summary, the results presented in this study indicate that the introduction of carboxylic acid substituents at polythiophene or oligomers based on thiophene produces a very small increase in the ϵ_g gap. More specifically, polymers based on the substitution patterns used for **n-1a** and **n-2ad** are expected to have electronic properties similar to those of unsubstituted polythiophene. These results are especially relevant to design water-soluble conducting organic polymers, which is a topic of broad interest in biotechnology.

Acknowledgements

Authors are indebted to CESCA (Centre de Supercomputació de Catalunya), CEPBA (Centre Europeu de Paral·lelisme de Barcelona) for computational facilities. This work was supported by MCYT and FEDER funds (project MAT2003-00251).

References

- [1] Roncali J. *Chem Rev* 1997;97:173.
- [2] Skotheim TA, Elsenbaumer RL, Reynolds JR, editors. *Handbook of conducting polymers*. 2nd ed. New York: Marcel Dekker; 1998.
- [3] Granstrom M. *Polym Adv Technol* 1997;8:424.
- [4] Miller GG, Elsenbaumer RL. *J Chem Soc, Chem Commun* 1986;169.
- [5] Garnier F. *Angew Chem, Int Ed Engl* 1989;28:513.
- [6] Chen TA, Wu X, Rieke RD. *J Am Chem Soc* 1995;117:233.
- [7] Roncali J, Garreau R, Delabouglise D, Garnier F, Lemaire M. *Synth Met* 1989;28:C341.
- [8] Souto Maior RM, Hinkelman K, Eckert H, Wudl F. *Macromolecules* 1990;23:1268.
- [9] Bartlett PN, Dawson DH. *J Mater Chem* 1994;4:1805.
- [10] Demanze F, Yassar A, Garnier F. *Adv Mater* 1995;7:907.
- [11] Kim B, Chen L, Gong J, Osada Y. *Macromolecules* 1999;32:3964.
- [12] Rasmussen SC, Pickens JC, Hutchison JE. *Macromolecules* 1998;31:933.
- [13] Kim Y-G, Samuelson LA, Kumar J, Tripathy SK. *J Macromol Sci* 2002;A39:1127.
- [14] Rasmussen SC, Pickens JC, Hutchison JE. *Chem Mater* 1998;10:1990.
- [15] Kim B-S, Fukuoka H, Gong JP, Osada Y. *Eur Polym J* 2001;37:2499.
- [16] Masuda H, Kaeriyama K. *Makromol Chem, Rapid Commun* 1992;13:461.
- [17] McCullough RD, Ewbank PC, Loewe RS. *J Am Chem Soc* 1997;119:633.
- [18] Pomerantz M, Cheng Y. *Tetrahedron Lett* 1999;40:3317.
- [19] Pomerantz M, Cheng Y, Kasim RK, Elsenbaumer RL. *Synth Met* 1999;101:16.
- [20] Pomerantz M, Amarasekara AS, Rasika Dias HV. *J Org Chem* 2002;67:6931.
- [21] Becke AD. *J Chem Phys* 1993;98:1372.
- [22] Perdew JP, Wang Y. *Phys Rev* 1992;45:13244.
- [23] Frich MJ, Pople JA, Krishnam R, Binkley JS. *J Chem Phys* 1984;80:3264.
- [24] Schmidt MW, Baldrige KK, Boatz JA, Elbert ST, Gordon MS, Jensen JH, et al. *J Comput Chem* 1993;14:1347 [PC-GAMESS supplied by A. Granovsky, Moscow State University].

- [25] Gaussian 98, Revision A.7, Frisch MJ, et al. Gaussian Inc., Pittsburgh, PA; 1998.
- [26] Koopmans T. *Physica* 1934;1:104.
- [27] Janak JF. *Phys Rev* 1978;8:7165.
- [28] Levy M, Nagy Á. *Phys Rev* 1999;59:1687.
- [29] Bernadó P, Alemán C, Puiggali J. *Macromol Theory Simul* 1998;7: 659.
- [30] Gould IR, Kollman PA. *J Phys Chem* 1992;96:9255.
- [31] Navas JJ, Alemán C, Muñoz-Guerra S. *J Phys Chem* 1995;99:17653.
- [32] Kobayashi M, Chem J, Chung T-C, Moraes F, Heeger AJ, Wudl F. *Synth Met* 1984;9:77.
- [33] Chung T-C, Kaufman JH, Heeger AJ, Wudl F. *Phys Rev B* 1984;30: 702.